

Shape Instabilities in the Dynamics of a Two-component Fluid Membrane

P. B. Sunil Kumar and Madan Rao

Institute of Mathematical Sciences, Taramani, Chennai (Madras) 600 113, India
(November 28, 2017)

We study the shape dynamics of a two-component fluid membrane, using a dynamical triangulation monte carlo simulation and a Langevin description. Phase separation induces morphology changes depending on the lateral mobility of the lipids. When the mobility is large, the familiar labyrinthine spinodal pattern is linearly unstable to undulation fluctuations and breaks up into buds, which move towards each other and merge. For low mobilities, the membrane responds elastically at short times, preferring to buckle locally, resulting in a crinkled surface.

PACS: 87.22.Bt, 64.60.Cn

A mixture of phospholipid molecules, e.g. DMPC + SOPC, aggregate in an aqueous solvent to form closed bilayered fluid membranes of dimension $10 - 20 \mu\text{m}$. Such mixed vesicles exhibit definite equilibrium shapes depending on the ambient temperature, osmotic pressure, relative concentration and history of preparation. Amongst the multitude of equilibrium shape transitions predicted by theory [1,2] and observed in phase contrast video micrography, the most dramatic is the phase segregation induced budding [1] at which a large ‘parent’ vesicle sprouts out a spherical bud consisting of one of the lipid species, attached to it by a narrow umbilical. Such equilibrium budding has been observed in a mixture of natural brain (sphingomyelin) lipids [3].

Apart from these equilibrium studies, there has been relatively little work on the dynamics [4] of mixed fluid membranes [5,6]. In the context of a 2-component fluid membrane undergoing phase separation, the study of nonequilibrium shapes becomes essential, since the lateral diffusion coefficient of lipids $10^{-8} - 10^{-7} \text{cm}^2/\text{sec}$, are such that the time scale over which local lipid concentration relaxes is comparable to shape relaxation times. In this Letter we study the shape dynamics of a 2-component, open fluid membrane experiencing phase separation, using both a dynamical triangulation monte carlo simulation (DTMC) and a Langevin description.

The shape dynamics of a 2-component fluid membrane involves 6 slow variables, the conserved total lipid density $\rho = \rho_A + \rho_B$, the conserved relative concentration $\phi = (\rho_A - \rho_B)/\rho$, the ‘broken symmetry’ shape variable $\mathbf{R}(u_1, u_2)$, and the total momentum density $\vec{\pi}$, which involves both lipid and solvent hydrodynamics. The primary dissipation mechanisms arise from the in-plane lipid viscosity and out-of-plane solvent viscosity [7]. We include the effects of solvent hydrodynamics in our Langevin analysis, but not in our DTMC.

Over length scales larger than the bilayer thickness ($d \sim 40 \text{\AA}$), a 2-component fluid membrane can be described by a continuum hamiltonian [1,2] $\mathcal{H} = \mathcal{H}_c + \mathcal{H}_{c-\phi} + \mathcal{H}_\phi + \mathcal{H}_\rho$, where the curvature energy [8], written in terms of the extrinsic curvature H reads ($g \equiv \det(g_{ij})$, where g_{ij} is the metric)

$$\mathcal{H}_c + \mathcal{H}_{c-\phi} = \kappa_c \int (H - H_0(\phi))^2 \sqrt{g} d^2u, \quad (1)$$

while \mathcal{H}_ϕ takes the usual Landau-Ginzburg form,

$$\mathcal{H}_\phi = \int \left[\frac{\sigma}{2} (\nabla \phi)^2 - \frac{\phi^2}{2} + \frac{\phi^4}{4} \right] \sqrt{g} d^2u. \quad (2)$$

The spontaneous curvature $H_0(\phi) = c_0(1 + \phi)/2$, reflects the shape asymmetry between the two lipid species, and biases the local curvature to be c_0 or 0. The upper length scale cutoff is set by the persistence length $\xi_p \approx d \exp(4\pi\kappa_c/3k_B T)$, beyond which thermal fluctuations drive the membrane into a self-avoiding branched polymer phase ($\kappa_c \approx 100k_B T_{\text{room}}$ for DMPC). In principle κ_c depends on the local concentration ϕ , but we shall ignore this detail (which allows us to drop the intrinsic curvature term usually present in Eq. 1). The energy cost for density fluctuations $\delta\rho$ along the membrane is $\mathcal{H}_\rho = \chi_0^{-1} \int (\delta\rho/2)^2 \sqrt{g} d^2u$ (where χ_0/ρ_0^2 is the compressibility of the membrane).

Our model 2-component membrane [5] consists of a fixed number N of two types of hard beads A and B (vertices), each of diameter a , with $N = N_A + N_B$, linked together by flexible tethers so as to triangulate a 2-dim open surface embedded in \mathcal{R}^3 . The length of each tether lies between $a = l_{\min} < l < l_{\max} = \sqrt{3}a$ (imposes self-avoidance locally [9]). The coordination number of every bead is restricted to lie between 3 and 9. The configurations of our model 2-component membrane are weighted by the discrete form of \mathcal{H} . The discretised curvature energy Eq. 1 is written as

$$\begin{aligned} & \kappa_c \sum_i \sum_{(ij)} \left[H_{(ij)} + \frac{K_i}{\sqrt{3}} \right] + \kappa_0^2 \kappa_c \sum_i \frac{(1 + \phi_i)^2}{4} a_i \\ & - \kappa_0 \kappa_c \sum_i (\pm) \sqrt{\sum_{(ij)} \left[H_{(ij)} + \frac{K_i}{\sqrt{3}} \right] (1 + \phi_i)}, \end{aligned} \quad (3)$$

where the index i denotes a vertex, (ij) the tether connecting i and j and $\sum_{(ij)}$ the sum over all tethers emanating from i . The term $H_{(ij)} = 1 - \hat{\mathbf{n}}_\alpha \cdot \hat{\mathbf{n}}_\beta$, where $\hat{\mathbf{n}}_\alpha$ and $\hat{\mathbf{n}}_\beta$ are the local *outward* normals to the triangles α

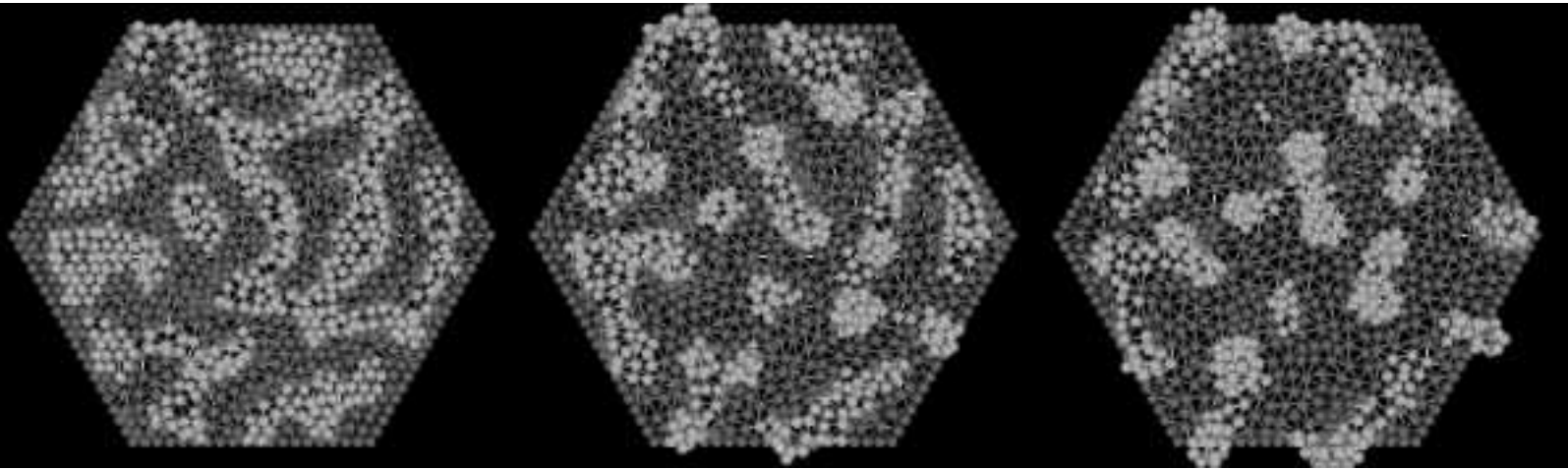


Fig. 1 Configuration snapshots from the DTMC simulation at times $t = 4000, 6500, 17000$ in units of MCS, for a critical quench. The number of particles is $N = 1140$, and the number of flips is $N_f = 15N$. The labyrinthine pattern, typical of spinodal decomposition, break up into buds at late times.

and β sharing a common tether (ij). The intrinsic curvature K_i , calculated from the deficit angle at i , must be added to $H_{(ij)}$ to obtain Eq. 1 in the continuum limit. The \pm sign in the third term, denotes the sign of the local mean curvature — it is positive if the *outward* normals to adjacent triangles point away from each other and negative otherwise. The concentration ϕ_i takes values ± 1 depending on whether the vertex i is occupied by A or B. In the second term of Eq. 3, a_i is the sum of the areas of the triangles with i as the vertex. The discrete version of Eq. 2 is clearly,

$$\mathcal{H}_\phi = -J \sum_{\langle ij \rangle} \phi_i \phi_j, \quad (4)$$

where the sum $\langle ij \rangle$ is over vertex pairs connected by a tether. Finally, \mathcal{H}_ρ is contained in our imposition of the hard sphere and tether constraints.

The DTMC for a 2-component fluid membrane consists of bead movements in \mathcal{R}^3 to change the shape [9], tether flips to simulate fluidity (dynamical triangulation) [9], and exchange moves between A and B to promote phase segregation [5]. Moves which violate the hard sphere and tether constraints, graph planarity (no tether intersections) and topology of the surface [9] are rejected. The bead moves and the tether flips are made according to a Metropolis algorithm with the hamiltonian Eqs. 3, 4. The exchange moves between A and B are implemented by the usual Kawasaki dynamics [10], with a transition probability $W(i \leftrightarrow j) = [1 - \tanh(\Delta E/2k_B T)]/2$, where ΔE is the energy difference between the final and the initial configuration. One monte carlo sweep (MCS) is defined as N attempted bead moves, during which we make N_f attempts at flipping tethers and N_{ex} attempts at Kawasaki exchanges. We shall work with two different boundary conditions — rigid boundary conditions

on a hexagonal frame (fixes the projected area) and free boundary conditions (unframed), in either case the tethers along the boundary are not flipped. Details of this algorithm may be found in [5].

A variant of this algorithm was used to study the phase separation dynamics of dense binary fluids confined to two dimensions [11]. The growth laws and the form of the correlation functions were consistent with a variety of other simulations [12]. We note that the lateral mobility of the beads may be tuned by N_f .

At time $t = 0$, we start with a homogeneous mixture ($N_A = N_B = N/2$; $N = 1140$) of A and B lipids on a flat, randomly triangulated 2-dim surface. After a quench into the coexistence regime [13], the fluid membrane evolves by the monte carlo dynamics just discussed. We shall investigate the generic case when the time scales, τ and τ_ϕ , over which the shape and the concentration change are comparable ($N_{ex} = N$), relegating a more detailed analysis to later [14]. The values of parameters have been chosen to be $J = \kappa_c = \kappa_0 = 1$ in units of $k_B T = 0.25$.

Before showing the sequence of monte carlo configurations, let us discuss the very early time spinodal instability, when we are justified in using a Monge parametrization of the surface $\mathbf{R}(u_1, u_2; t) \equiv (x, y, h(x, y; t))$. The continuum Langevin equations of motion for h and ϕ read,

$$\frac{\partial \phi}{\partial t} = -c_0 \nabla^4 h - \sigma \nabla^4 \phi - \nabla^2 \phi + 3\phi^2 \nabla^2 \phi + 6\phi(\nabla \phi)^2 \quad (5)$$

$$\frac{\tau}{\sqrt{1 + (\nabla h)^2}} \frac{\partial h}{\partial t} = -\kappa_c \nabla^4 h + c_0 \nabla^2 \phi. \quad (6)$$

We perform a linear stability analysis about a flat membrane with $h(\mathbf{x}, t) = \sum_{\mathbf{q}} \delta h_{\mathbf{q}}(t) e^{i\mathbf{q} \cdot \mathbf{x}}$ and $\phi(\mathbf{x}, t) = \phi_0 +$

$\sum_{\mathbf{q}} \delta\phi_{\mathbf{q}}(t)e^{i\mathbf{q}\cdot\mathbf{x}}$. The overdamped modes are unstable for $q < q^*$, where $q^* = \sqrt{(1 - 3\phi_0^2 + c_0^2/\kappa_c)/\sigma}$. The small q dispersion of the unstable mode is easily worked out — $\omega \sim q^2$ for $\phi_0^2 < 1/3$ and $\omega \sim q^4$ for $\phi_0^2 > 1/3$. Solvent hydrodynamics, introduced through a renormalized $\tau \sim (\eta q)^{-1}$ (η = solvent kinematic viscosity), changes the q^4 dispersion to $\omega \sim q^5$, leaving the other features unaffected. The coupling to shape fluctuations shifts the (mean field) spinodal line closer to the coexistence line: $\phi_0^2 = 1/3 + c_0^2/3\kappa_c$. The configuration coarsens into the usual labyrinthine pattern, Fig. 1(a), which is a snapshot from our DTMC at $t = 4000$ MCS.

Subsequent evolution depends on the magnitude of the lateral mobility. Let us first consider the case when $N_f = 15N$, which corresponds to mobile lipids in the fluid phase. A look at a time sequence of configurations generated by our simulation Fig. 1, reveals an unusual scene. The bicontinuous patches, which are a generic feature of binary fluids at a critical quench, break up into disconnected buds as time progresses! Further coarsening occurs through the motion of these buds, as they approach each other and subsequently coalesce. The late time behaviour depends on the final equilibrium configuration of the membrane.

To understand the breakup of the bicontinuous patches (strip instability), we again work within the Monge gauge and perform a linear stability analysis about a flat strip of width $2u_0$ with $\phi = 1$ within the strip and $\phi = -1$ without. We parametrise the perturbed configuration by $h = h_0 + \sum_{\mathbf{q}} \delta h_{\mathbf{q}}(t)e^{i(q_1x + q_2y)}$ and $\phi = \tanh[(u(x, t) - y)/\xi] + \tanh[(u(x, t) + y)/\xi] - 1$, where $u(x, t) = u_0 + \sum_{q_1} \delta u_{q_1}(t)e^{iq_1x}$ and $\xi = \sqrt{2\sigma}$ is the interfacial thickness. The time evolution of the fourier amplitudes evaluated at $y = \pm u_0$ is, to linear order,

$$\begin{bmatrix} \delta \dot{u}_{q_1} \\ \delta \dot{h}_{q_1} \end{bmatrix} = \begin{bmatrix} -\sigma q_1^4 - 4q_1^2 & -\sqrt{2\sigma}c_0q_1^4 \\ -\frac{c_0}{\tau\sqrt{2\sigma}}(\frac{1}{\sigma} + q_1^2) & -\frac{\kappa_c}{\tau}q_1^4 \end{bmatrix} \begin{bmatrix} \delta u_{q_1} \\ \delta h_{q_1} \end{bmatrix}. \quad (7)$$

Such a perturbation leads to a long wavelength instability of the strip. The dispersion of the unstable mode is $\omega \sim q_1^2$, as $q_1 \rightarrow 0$. Hydrodynamic coupling to the solvent via a renormalized $\tau(q)$ does not alter this dispersion. This instability, arising from a competition between the interfacial and the curvature energy [1], leads to local outward budding since $c_0 > 0$. This linear instability will grow into the complete buds seen in Fig. 1(c), connected to the rest of the membrane through a narrow neck. The typical size of the bud is $R_H = \kappa_c/(c_0 + \sigma)$. The $c_0 = 0$ case is special since the linear analysis does not predict a strip instability; nonlinear terms however would initiate an instability to budding. Since the bud could form either outward or inward, the dynamics of bud formation is logarithmically slow as can be seen by a mapping onto a 1-dim, scalar time-dependent Ginzburg-Landau (TDGL) dynamics [10].

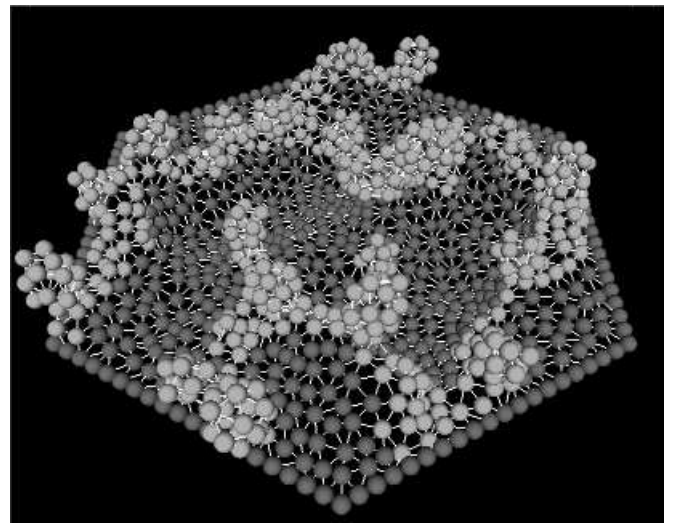


Fig. 2 Configuration snapshot from the DTMC simulation at $t = 17000$ MCS for a critical quench. The number of particles is the same as in Fig. 1, but $N_f = N$. The late time configuration is now ‘crinkled’.

When the mobility is small ($N_f = N$), the intermediate time shapes are dramatically different. Instead of erupting buds, the membrane develops sharp ridges at the A|B interface and appears *crinkled* (Fig. 2). We argue that these crinkles are a consequence of a disclination induced *buckling* instability. The A|B interfacial energy can be reduced both by shrinking the interface perimeter and by lowering the local coordination number of the beads at the interface. This introduces a preponderance of positive orientational disclination defects at the interface, in an otherwise 6-fold coordinated network. Though the membrane is still in the fluid phase [15], the high lipid viscosity η_l results in a nonzero shear modulus $\mu \sim \eta_l/\tau_s$ over time scales smaller than the shear relaxation time τ_s [16]. The membrane therefore responds elastically to the presence of these disclinations. Placing a positive disclination on a flat elastic sheet of size R costs an energy proportional to K_0R^2 , where $K_0 = 4\mu(\mu + \lambda)/(2\mu + \lambda)$ is related to the elastic moduli. Buckling eliminates the elastic contributions to the stress field created by this defect [17], leaving only a bending energy cost which goes as $\kappa_c \ln R$. As shown in [17], the elastic membrane buckles when $K_0R^2 \geq 160\kappa_c$. This physics is consistent with our monte carlo shape evolution of a flat membrane having a single patch of A in a sea of B lipids with $N_f = N$. The membrane goes into a *buckled* conical shape, with the A species at the tip. This buckled shape is clearly a long-lived nonequilibrium effect. The same elastic considerations would imply that negative disclinations would induce a long-lived negatively curved (saddle) buckled surface. The relative fraction of positive and negative disclinations depends on the boundary conditions at the frame. Unless there is an excess charge, either due to

initial conditions or by having an open boundary, the membrane will be asymptotically flat. The crinkled look of Fig. 2 is a consequence of a random distribution of such positively and negatively buckled surfaces.

The dynamics of coarsening and shape changes can be studied from the behaviour of a variety of two-point correlators. We define as R_E , the length scale associated with the interfacial energy density, $\langle E \rangle = N^{-1} \sum_{\langle i,j \rangle} (1 - \phi_i \phi_j)$, and R_H , the length extracted from the total mean curvature density $\langle H \rangle = N^{-1} \sum_i (\pm) \sqrt{\sum_{\langle ij \rangle} [H_{ij}] + \frac{K_i}{\sqrt{3}}}]$. In addition, we measure $R_{\phi\phi}$ from the first zero of the intrinsic equal-time correlator for the local concentration $\Gamma_i(r_2, t) \equiv \frac{1}{N} \sum_{\mathbf{u}} \langle \phi(\mathbf{u} + \mathbf{r}_2, t) \phi(\mathbf{u}, t) \rangle$ and R_{HH} from the first zero of the intrinsic equal-time correlator for the local curvature $\Delta_i(r_2, t) \equiv \frac{1}{N} \sum_{\mathbf{u}} \langle H(\mathbf{u} + \mathbf{r}_2, t) H(\mathbf{u}, t) \rangle$, where $|r_2|$ is the geodesic distance between points \mathbf{u} and $\mathbf{u} + \mathbf{r}_2$ defined on the 2-dim manifold. Geodesic distances are computed using Floyd's algorithm for a directed graph [18]. As might be expected from the absence of self-similarity in Fig. 1, we do not observe dynamical scaling in the above correlators over the time scales of our simulation.

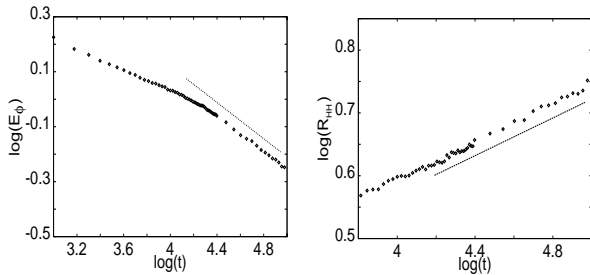


Fig. 3 Growth laws extracted from the DTMC with $N_f = 15N$ (the straight line fits are aids to the eye). (a) $R_E \sim E_\phi^{-1}$ crosses over to the usual $t^{1/3}$ growth, while (b) R_{HH} exhibits a late time $t^{1/6}$ behaviour.

The length scales R_E , R_H and R_{HH} (averaged over 16 runs) are displayed in Figs. 3(a) and 3(b) for $N_f = 15N$ ($R_{\phi\phi}$ behaves the same as R_E). We identify two dynamical regimes associated with distinct growth processes. Regime I heralds the initiation of the strip instability to the formation of buds and the length scales, R_E , R_H and R_{HH} grow as $t^{1/4}$ [5]. This is followed by regime II where the buds of typical size R_H move towards each other and subsequently coalesce. In the absence of any hydrodynamic drag due to the solvent, $R_E \sim t^{1/3}$. This dependence will be unchanged by inclusion of a viscous drag due to the solvent (though the prefactor would be altered). The buds carry both ϕ and curvature H , and so equating the energy densities $E_\phi \sim R_E^{-1}$ and $E_H \sim R_{HH}^{-2}$, leads to $R_{HH} \sim R_E^{1/2} \sim t^{1/6}$ (Fig. 3(b)).

It would be interesting to carry out a systematic experimental study of dynamical morphology changes and shape instabilities in mixed artificial membranes. Of course the choice of the lipid species is crucial; it is important to ensure that $T_c > T_m$, the main transition temperature below which the lipid freezes into a gel state ($T_m \approx 23^\circ\text{C}$ for DMPC). This may be achieved by choosing lipids with short chains or with a lot of unsaturated bonds within the chain [19]. The dynamical buckling phenomenon reported above could be observed by inducing photochemical (UV) crosslinking of the minority lipids after they have clustered. The present study might be of relevance to biological membranes as well, in particular to the dynamics of ‘budding’ of coated vesicles and the ‘patching’ of membrane proteins and glycolipids [19].

- [1] R. Lipowsky, Biophys. J. **64**, 1133 (1993), J. Phys. II (France) **2**, 1825 (1992); F. Julicher and R. Lipowsky, Phys. Rev. Lett. **70**, 2964 (1993).
- [2] D. Andelman, T. Kawakatsu and K. Kawakatsu, Europhys. Lett. **19**, 57 (1992); U. Seifert, Phys. Rev. Lett. **70** 1335 (1993).
- [3] H. -G. Döbereiner *et. al.*, Biophys. J. **65**, 1396 (1993).
- [4] W. Cai and T. C. Lubensky, Phys. Rev. Lett. **73**, 1186 (1994); Phys. Rev. **E52**, 4251 (1995).
- [5] P. B. Sunil Kumar and M. Rao, <http://xxx.lanl.gov/archive/cond-mat/9603027>, Mol. Cryst. Liq. Cryst. **288**, 105 (1996).
- [6] T. Taniguchi, Phys. Rev. Lett. **76**, 4444 (1996).
- [7] We ignore friction between the bilayer leaves, which provides an additional dissipative mechanism at long length scales, A. Seung and E. Evans, Euro. Phys. Lett. **23**, 71 (1993); U. Seifert and S. Langer, Euro. Phys. Lett. **23**, 71 (1993).
- [8] P. B. Canham, J. Theor. Biol. **26**, 61 (1970); W. Helfrich, Z. Naturforsch. Teil C **28**, 693 (1973); E. Evans, Biophys. J. **14**, 923 (1974).
- [9] A. Baumgärtner and J. -S. Ho, Phys. Rev. **A41**, 5747 (1990); D. Boal and M. Rao, Phys. Rev. **A45**, R6947 (1992); D. Kroll and G. Gompper, Phys. Rev. **A46**, 3119 (1992).
- [10] A. J. Bray, Adv. Phys. **43**, 357 (1994).
- [11] P. B. Sunil Kumar and M. Rao, Phys. Rev. Lett. **77**, 1067 (1996).
- [12] W. R. Osborn *et. al.*, Phys. Rev. Lett. **75**, 4031 (1995); E. Velasco and S. Toxvaerd, Phys. Rev. **E54**, 605 (1996).
- [13] The critical temperature $T_c \rightarrow 0$ in the thermodynamic limit, since for sizes $L \gg \xi_p$, the membrane behaves like a self-avoiding branched polymer, with the lipids sitting on the boundary. For DMPC membranes, however, ξ_p is fairly large.
- [14] P. B. Sunil Kumar and M. Rao (to be published).
- [15] The presence of a number of isolated disclinations, and a structureless $\langle n_5(r)n_7(0) \rangle$ (n_5 and n_7 are the densities of the 5- and 7- membered rings respectively), imply that

the membrane is not in the hexatic phase.

- [16] L. D. Landau and E. M. Lifshitz, in *Theory of Elasticity*, 3rd Edition, Pergamon Press (1986).
- [17] S. Seung and D. R. Nelson, Phys. Rev. **A38**, 1005 (1988) ; D. C. Morse and T. C. Lubensky, Phys. Rev. **A46**, 1751 (1992) ; D. R. Nelson and L. Radzhidovsky, Phys. Rev. **E46**, 7474 (1992) ; D. R. Nelson, in *Fluctuating Geometries in Statistical Physics and Field Theory*, NATO ASI, Les Houches (1994).
- [18] G. Brassard and P. Bratley, in *Algorithmics*, Prentice Hall (1988).
- [19] B. Alberts *et. al.*, in *Molecular Biology of the Cell*, Garland Publ. (1989).